Mansoura Engineering Journal

Volume 35 | Issue 2 Article 5

11-21-2020

Relationship between Visual Cavitation Inception and 3% Drop in Head in Centrifugal Pumps.

M. Hosien
Mechanical Power Engineering Department ., Faculty of Engineering

S. Selim
Minoufiya University, Shebin El -Kom, Egypt

RELATIONSHIP BETWEEN VISUAL CAVITATION INCEPTION AND 3 % DROP IN HEAD IN CENTRIFUGAL PUMPS

العلاقة بين بداية حدوث التكهف المرئى وانخفاض العلو بمقدار 3 % للمضخات الطاردة المركزيه

M.A.Hosien*and S.M.Selim**

Department of Mechanical power Engineering, Faculty of Engineering
Minoufiya University, Shebin El –Kom, Egypt

تصمم وتصنع المضخات للعمل بعيدا عن حدوث التكهف. عرف المصمم بداية حدوث التكهف فى المضخات بالنقطة التى يحدث عندها انخفاض فى العلو بمقدار 3% ، وهذا التعريف غير صحيح، حيث أن بداية ظهور فقاعات بخار السائل تحدث قبل هذا الانخفاض بكثير. ان اعتبار انخفاض العلو بمقدار 3% دليل بداية ظهور التكهف يؤدى الى انهيار أداء المضخة.

تناول هذا البحث دراسة تجريبية لحساب علو السحب الموجب الصافى بناءا على المشاهدة وذلك عند معدلات تدفق ،سرعات دوران ودرجات حرارة مختلفة. كما تم اخذ صور فوتوغرافية عند أوضاع تشغيل مختلفة وذلك لتوضيح حقيقة حدوث وشكل التكهف عند كل حاله.

من خلال هذه الدراسة تم إيجاد علاقة بين علو السحب الموجب الصافى المبنى على المشاهدة المرئية وعلو السحب الموجب الصافى المناظر لهبوط العلو بنسبة 3 % تم فيها الأخذ فى الاعتبار جميع المتغيرات التى تم دراستها عمليـــا.

ABSTRACT

Pumps were designed and manufactured to operate far from the cavitation condition. Pump designer has defined the cavitation inception point as the point where the head drops by 3 %. This definition is incorrect, because the first appearance of vapour bubbles was observed earlier than 3 % drop in the head. Therefore using 3 % drop in head, as indication parameter for cavitation inception has always resulted in damage in pumps during operation. This paper describes visual studies conducted to determine the variation of net positive suction head with flow rate, rotational speed and water temperature. A special correlation between the visual net positive suction head and net positive suction head corresponding to 3 % drop in head was predicted at various operating conditions.

Keywords: Cavitation inception, Net Psitive Suction Head, Visualization.

1. INTRODUCTION

The present study was intended to investigate visually the changes in flow rate, suction pressure, rotational speed and temperature of a pumped water on the cavitation performance of centrifugal pumps. These factors are generally termed "thermodynamic and thermodynamic effects" and studies on these aspects are numerous and comprehensive. For pump designers, knowledge of the cavitation phenomenon is very important for proper design. Some pump designers have defined the critical cavitation coefficient as the point where the head drops by 3 percent. This is because it was believed that if the performance was not affected no cavitation occurred and that the head first started to drop was the point of cavitation inception. This definition does not show the real state of cavitation inception in the pump, and that incipient of cavitation may exist long before the performance is affected [1]. At this point where the head drops by 3 % cavitation erosion was noticed. Reliance on this definition can cause errors in the prediction of efficiency and performance at the design stage. Therefore, there is clearly

* Lecturer ** Professor

Accepted June 30, 2010.

need for reliable data on the variation of visual net positive suction head and NPSH corresponding to 3 % drop in head at various operating conditions with a view to develop possible relationships between them.

El-Kadi [2] has studied the cavitation in a centrifugal pump handling hot water from (28°C to58°C). The suction side of the pump was made of transparent perspex material in order to notice out the cavitation degree at the corresponding flow condition, but no correlation between visual net positive suction head and net positive suction head corresponding to 3%drop in head was noticed. Hirschi et al, [3] have carried out a numerical prediction in the performance drop of centrifugal pumps due to leading edge cavitation. The carried work was complicated, and the results obtained with a new 3-D numerical method. This prediction based on 2-D profile done by Yamaguchi and Kato on (1983). The influence of pressure distribution, cavity lengths and the diffuser geometry on the performance drop of cavitating flow were studied using 3D Navier-Stockes and Rayleigh -Plesset equation, and they finally compared the prediction results with the test results. It was concluded that 3-D Navier-Stockes computation gave a very well comparison in behavior of cavitating flow in centrifugal pumps between predicted and measured results. The difference of pressure distribution corresponds to cavitation inception was determined for all calculated points and the deviation between the measured and calculated points was found less than 4 %. The cavity length computation provides very good results. It was concluded also that the turbulence losses have a remarkable effect on the performance drop. The behavior difference between diffusers was mainly due to unsteady phenomenon or cavitation development in the diffuser. Donald P. Sloteman, [4] has studied the cavitation in high energy centrifugal pump for detecting and assessing the damage potential. The detection of cavitation was based on the noise and visualization technique measurements. He reported sufficient information about the acoustic technique used by the previous researchers. For noise level measurements a waveform of sex different sensors positioned very nearly in phase has been used, and a special transparent window was made on the pump for flow visualization. It was observed that changes in cavitation level can be measured at many locations on the pump and piping. He concluded that there still is a need for detection tools that can serve aftermarket concerns of pumps already in the field and that also can be applied to new design optimization efforts of manufacturers while on the test stand. Detlev L. Wulff, [5] introduced an overview on the basic principles of Digital Particle Imaging Velocimetry *(DPIV)* and the main components of standard systems. Special efforts were made to report on the particularities of measurements in stationary as well as rotating components of pumps. The used rig consists of a standard PC for controlling the Particle Image Velocimetry *(PIV)* processor and data post processing. Cameras and laser head were mounted separately on two stepper motor controlled 3-axis petitioners. The stereoscopic DPIV was set-up at the pump test rig and directed to the transparent window for visualization process. Using *DPIV* permits measurement of three velocity components, and recording different shapes of nuclei. With using PIV technique a compromise between spatial resolution and velocity resolution is required. A special and accurate photos have been taken at inlet section of the pump impeller, and

the local values of circumferential velocities on the impeller inlet with and without casing treatment were measured. L. Alfayez et al., [6] investigated the applications of acoustic emission for detecting incipient cavitation. They presented results from an on-going program to ascertain the applicability of the acoustic emission technique for determining the best efficiency point of an operating system. A large-scale pump rig (2.2MW) formed the basis of this investigation that included a series of NPSH and performance tests. They concluded that the results obtained demonstrate a successful use of acoustic emission technique for detecting incipient cavitation and identifying the best efficiency point a system employing pumps.

2. EXPERIMENTAL WORK

The flow system was designed and constructed according to the pump specifications in such a way that the pump must overcome the head losses in the system. The general arrangement of the test rig is indicated in a schematic diagram shown in figure 1. The flow system consists of 7.5 hp single stage centrifugal pump with a spiral casing of INTERSIGMA (NVA) series, 50 NVA-175-6 type. The specific speed of the pump (Ns) =1.87. The pump can handle water up to a temperature of 90°c. The type of the plain impeller of the pump is a closed impeller with six curved vanes. The inside and outside diameters of the impeller are 5.4 cm and 17.5 cm, respectively. The inlet and outlet blade angles are 21.5° and 28° respectively. The blade height at inlet and outlet are 10.5 mm and 5 mm, respectively. The pump performance characteristics were performed at different water temperature varies from 20°C to 90°C, and rotation speed varies from 2600 - 3000 rpm. The performance curves will be shown and discussed later. The pump inlet section was made of transparent perspex. The perspex face is connected with a perspex pipe of 5.08 cm inside diameter and 43 cm long in order to visualize any extension of swirling waves in the suction waves. The impeller front shroud was manufactured from transparent perspex to permit visual observation of cavitation inception. The outer surface of original impeller was removed gently in order to replace it by a perspex cover. The delivery and suction pipes were made of commercial steel pipes of 5.08 cm inside diameter. The main tank is manufactured from iron steel of 1 cm thick, 60 cm inner diameter and 120 cm height. The tank volume is 0.34 m^3. A special cooling coil to remove the dissipated energy in water from losses through valves, bends, coupling, etc, in the circuit. An electromagnetic flow meter was used to measure the volume flow rate. For more accurate flow rate measurements a special orifice was connected to a mercury manometer. Heat is supplied to the working fluid by three glass wool insulated Nicrome heater taps of 2 kW each wrapped around the lower end of the tank. To control the rotational speed a speed inverter of type (Hitachi LI00) has been used.

3. TEST CONDITIONS

The visual observation of inception, developed and breakdown cavitation conditions were conducted using stroboscopic light through the perspex cover of the pump. The suction static lift of 0.67 m was kept constant, and it was checked repeatedly during the tests. The flow rate ratio (Q/Q_{opt}) was varied from 0.3 to 1.1 with step of 0.1. The pump was operated at different rotational speeds of 1500, 1800, 2100, 2600, 2700, 2800, 2900 and 3000 rpm.

Water temperature was varied from 20°C to 90°C with a step of 10°C.

The experiments were carried out at fixed room temperature of 25 ± 1°C in order to obtain more accurate results.

1- Pump motor.
2- Pump.
3- Delivery valve.
4- By-pass line.
5- Electromagnetic flowmeter.
6- Orifice.
7- Main tank.
8-Electric heater
9- Main suction valve.
10- Control suction valve.
11- Speed inverter.
12- Suction pressure gauge.
13- Delivery pressure gauge.
14-U- tube manometer .

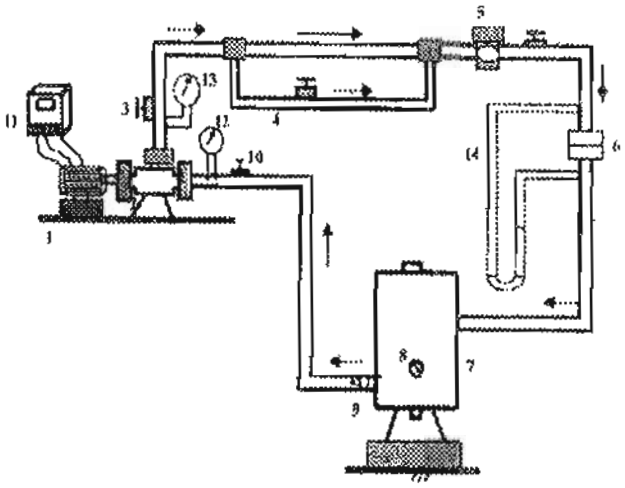

Fig.1. Cavitation test circuit.

4. RESULTS AND DISCUSSION

4.1 Visual Observation of Cavitation

Practical difficulties in cavitation testing and obtaining data from the vicinity of a rotating impeller have reduced the availability of consistent information on cavitation effects. The state of knowledge is such that quite fundamental effects may still be overlooked. As the pump is throttled up its characteristic the pressure in the suction peak region may drop below the vapour pressure resulting in strong local cavitation.

The purpose of this section is detailed photographic investigation of cavitation patterns in order to elucidate physical phenomena not previously observed or understood. A program of work was conducted using the existing pump rig which was provided with a transparent perspex casing for observation and photography. The observation of cavitation was achieved stroboscopically by eye and using Sony digital still camera (Model DSC-S70). Photographs of cavitation behaviour were obtained under a wide range of discharge throttle settings from wide open up to recirculatory condition. Figure 2 shows a series of photographs taken at various flow rates with constant rotational speed of 3000 rpm and temperature of 28 °C. At point (1) in which the delivery valve is fully open the breakdown of cavitation occurred and the cavity causing "shocking" of the channel between blades and appeared on both sides of the blades, the suction side and the pressure side and covered the impeller completely. A reduction in flow rate point (2) produces a large milky cavity moves on the surface of the blades and then moves with vortex towards the middle of the channel until it reaches a point adjacent to the opposite blade.

The liquid adjacent to the large-cavity surface has been observed to contain a multitude of small travelling transient cavities. As the flow rate was further reduced, point (3), the cavity decreased in its volume with decreasing the flow rate. The cavity observed was of milky appearance and of fluctuating length. Further reduction in flow rate point (4) the cavity appears to be a fixed sheet attached to the surface of the suction side of the blade. At point (4) the state of alternative cavitation was observed at 70% part load. The photograph (4) shows that there are two cells of fully developed pressure side cavitation within the impeller seperated by channel without cavity. With this observation, this can be understood as an impeller stability problem, which is driven by the increasing cavity length in relation to the incidence and the start of recirculatory flow at the inlet of the impeller. In this type of cavitation two adjacent channels are operating at different points of the impeller characteristic. The cavitating channel operates at a point with a lower flow rate ratio leading to an increase in the local incidence angle, while, the uncavitating channel operates at a higher flow rate ratio leading to a decrease in the local incidence angle. Consequently the lower flow rate ratio means a stronger pressure rise in the channel between blades and the higher flow rate ratio means a weaker pressure rise. The stronger pressure gradient suppresses the development of cavitation further into the channel while the depression of static pressure rise in the next channel allows cavity to grow in it. This may confirmed by the Hofmann et al. experimental results which indicated the occurrence of a periodic cavitation state called "rotating cavitation" in a wide range of part load conditions [7] Their results were obtained using a high technique photographic process with a 12-bit CCD-camera and a digital video camera operating in frame integrating mode with a frame-grabber device and both a stroboscopic light source and a laser-Light-Sheet-Technique used for illumination of the optical observation. For further reduction on the flow rate ratio point (5) and (6) the cavity appears as a cloud of small bubbles, the cloud grew and extended into the impeller passages. This cloud contains small bubbles have glassy appearance. This glassy appearance is due to the growth of gas bubbles by diffusion with cores of free vortex which is established outside the boundary layer surrounding the blade surface. Vortex type flows characteristically have high velocities near the vortex core with corresponding low pressure. The results of photograph in figure 3 show that the intensity of cavitation increases with the increase of rotational speed and this is mainly occurred due to the recirculatory flow, which increases with increasing the rotational speed. With further increase in the water temperature at T= 50°C the colour of the cavities changed gradually and becomes white with high brightness in colour and the cavities looks to be a cloud of continues linked bubbles as shown in figure 4. With further increase in the water temperature at T = 80°C the colour of the cavities becomes intermediate between the white and the glassy colour as shown in figure 5. Also at T = 80°C the bubbles will be elongated the shape and discontinuous clouds of cavities will be observed as shown in positions 2 and 3 in figure 5. The photographs results show that the cavitation covered most of the impeller channel at T = 80°C and N = 3000 rpm.

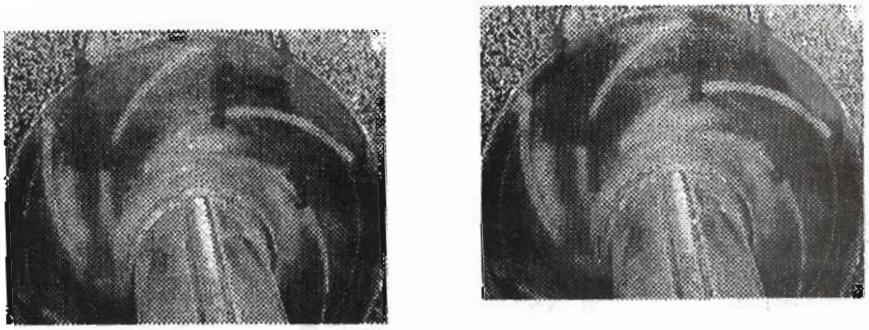

6

5

4

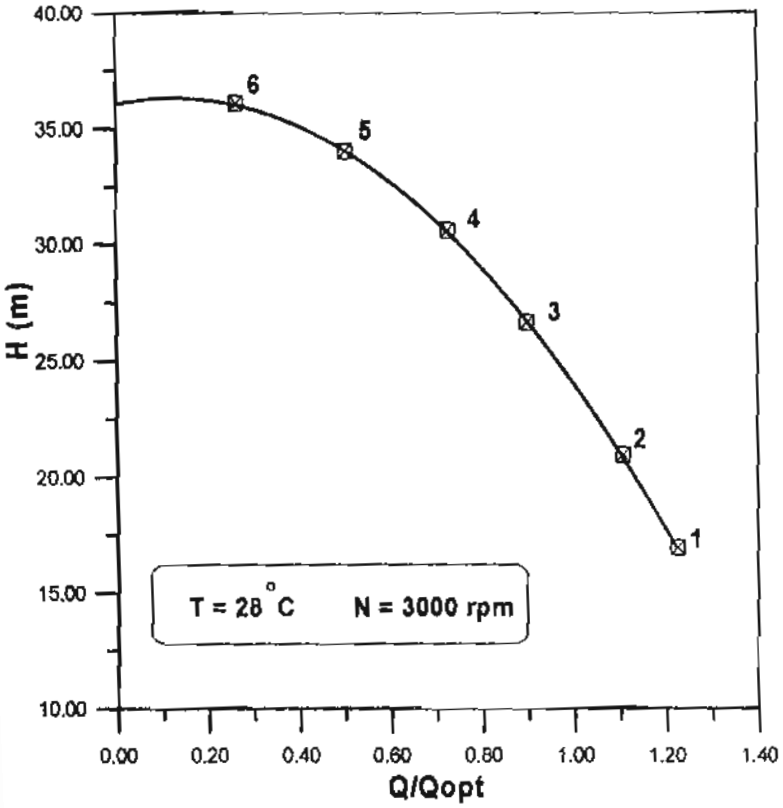

3

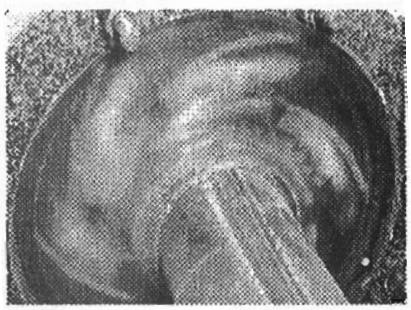

2

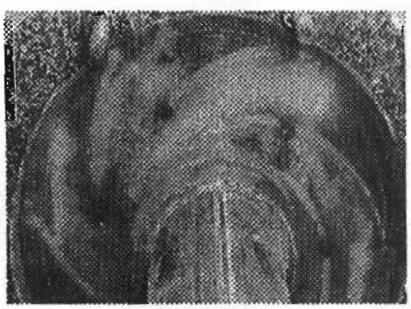

1

Fig. 2 Visulation of cavitation at various flow rate ratios

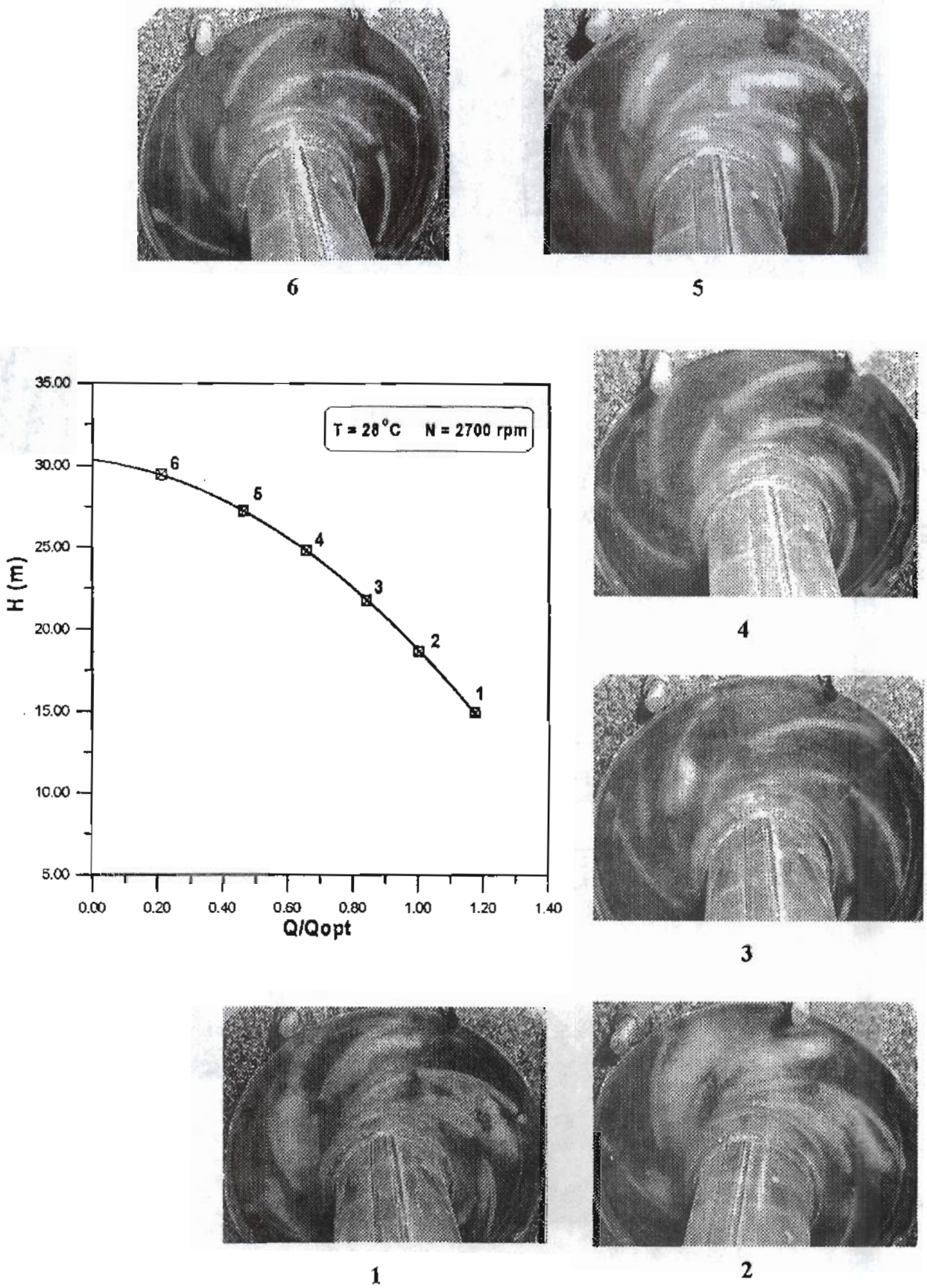

Fig. 3 Visulation of cavitation at various flow rate ratios

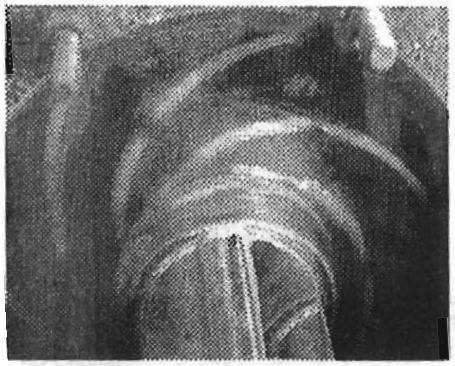

6

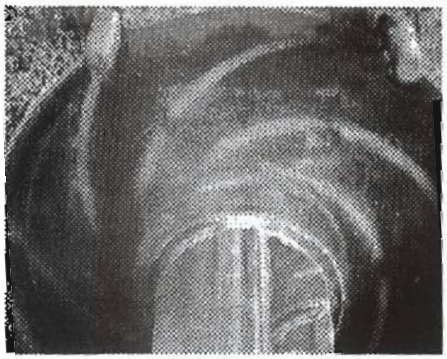

5

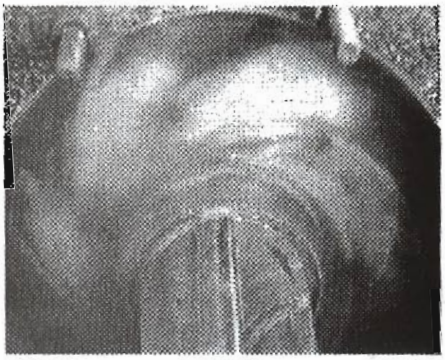

4

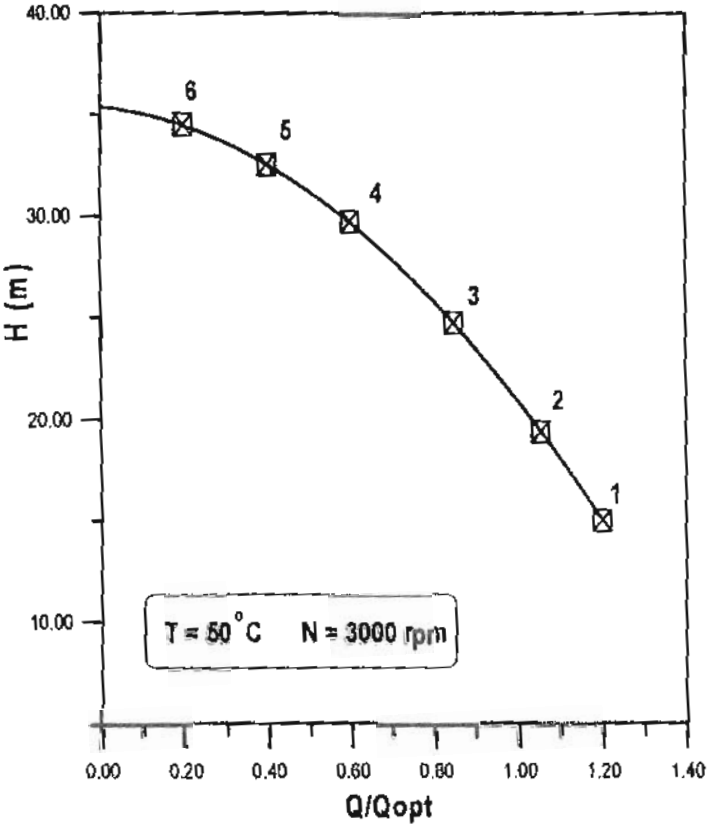

3

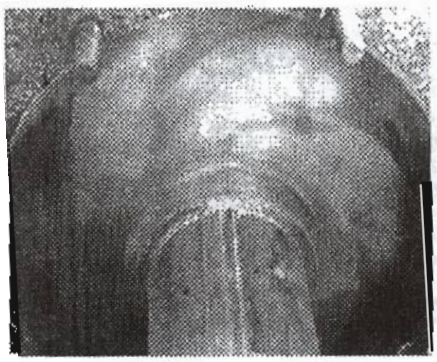

1

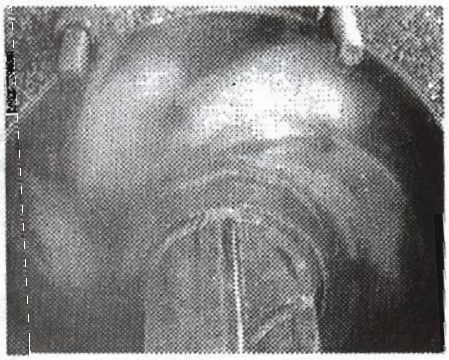

2

Fig. 4 Visulation of cavitation at various flow rate ratios

5

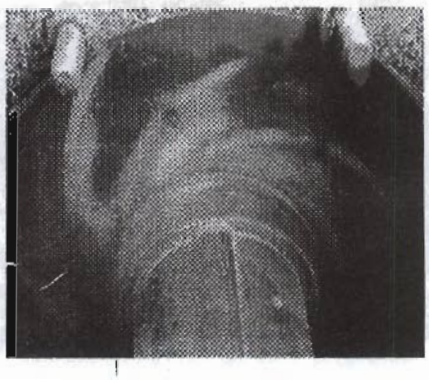

4

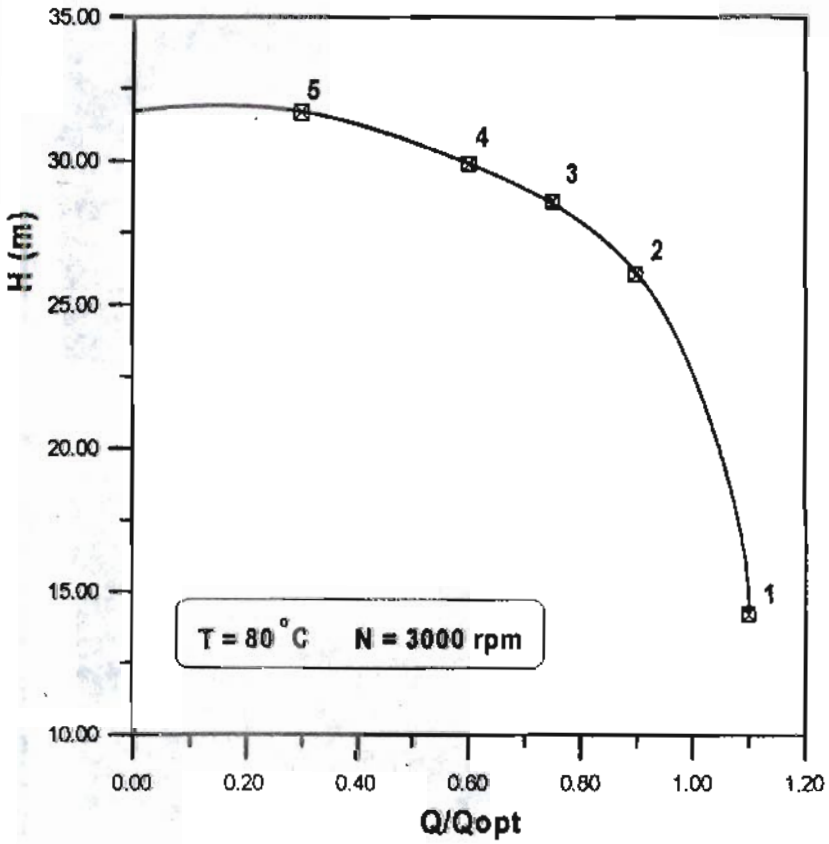

3

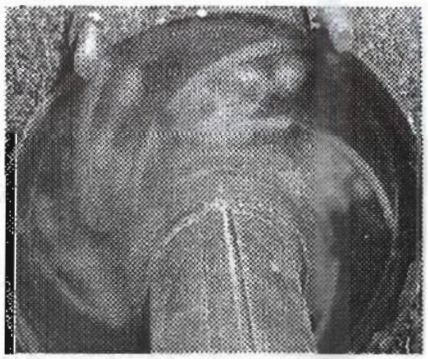

2

1

Fig. 5 Visulation of cavitation at various flow rate ratios

4.2 Visual Incipient Net Positive Suction Head

In this paper the major goal is to investigate experimentally, the effect of flow rate ratio, water temperature and the pump rotational speed on the visual incipient net positive suction head ($NPSH_i$). The visual inception cavitation refers to the first appearance of a limited cavitation zone at the leading edge of the blade of the pump. The inception condition was obtained by stroboscopic observation and by maintaining a constant flow rate while reducing the suction head. Predicting a relationship between visual $NPSH_i$ and the NPSH corresponding to 3 % drop in head will provide the pump designers with more accurate criterion of cavitation inception, and this will be very convenient to design and practical purposes. To achieve this purpose extensive series of experiments were carried out at various operating conditions. The results of the extensive series of experiments are shown in appendix A. Figure 6 shows the relation between the cavitation inception point and 3% drop in head.

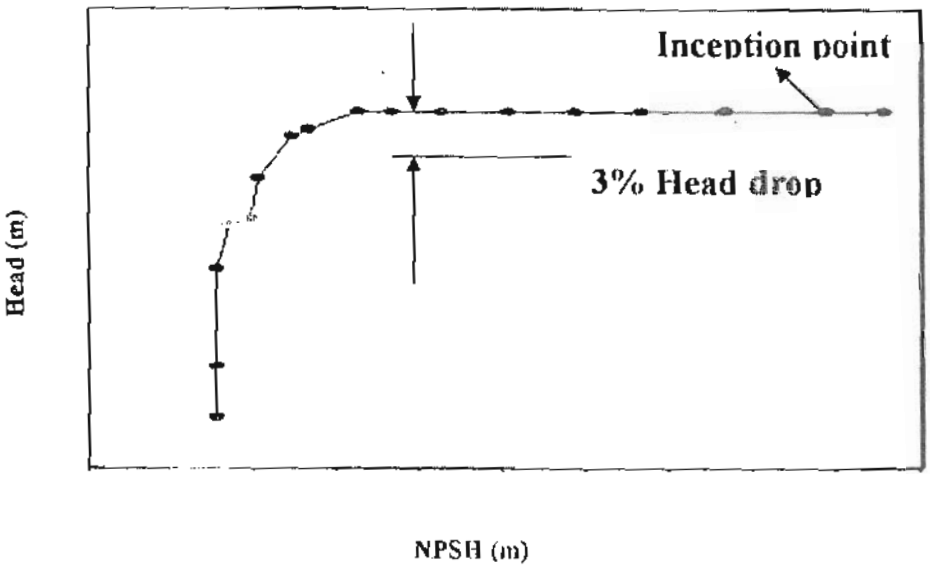

Fig. 6 Relation between the cavitation inception point and 3% drop in head.

4.3 Relation Between Visual NPSH and NPSH Corresponding to 3% Drop in Head

For pump designers, knowledge of the cavitation phenomenon is very important for proper design. Pump designers have defined the critical cavitation coefficient as the point where the head drops by 3 percent. This is because it was believed that if the performance was not affected i.e, no cavitation occurred and that the head first started to drop was the point of cavitation inception. The present results showed that, at this point where the head drops by 3 % sever cavitation erosion is most likely. Reliance on this definition can cause errors in the prediction of efficiency and performance at the design stage. Therefore, there is clearly a need for reliable data on the variation of visual net positive suction head and NPSH corresponding to 3 %drop in head at various operating conditions with a view to develop possible relationships between them.

Table I shows the reality of cavitation at 3 % head drop at constant Q/Q_{opt} = 0.4 and various water

temperatures and different rotational speeds. This table indicates that the inception condition commences long before the 3 % drop in head and developed cavitation is observed. Visual observation at 3 % drop in head shows that the length of cavity on the blade is varied from 25 % to 70 % of the blade length according to the test condition. Figure 7 shows photographs of the cavitation at a 3 % drop in head. It is appeared that at 3 % drop in head the pump is subjected to sever erosion that is detrimental to the life of the blades.

In analysing the results of cavitation tests, the relations between NPSHi,vis and NPSH3% were examined. The plots of $NPSH_{i,vis}$ against NPSH3% is shown in figure 8. This figure illustrates that the relationship between visual $NPSH_i$ and NPSH corresponding to 3% drop in head is independent of flow rate ratio and rotational speed. Nevertheless, it is dependent of the water temperature. This figure indicates that there is a very good relation between NPSHi,vis against NPSH3% for all the data. Equations for the regression lines were derived for figure 8, using the method of least squares. Values of the correlation coefficients and the regression lines are presented in table 2.

Table I: Reality of cavitation according to observation.

Parameters	T [°C]	N (rpm)	Q/Q_{opt}	$NPSH_{vi}$ (m)	$NPSH_{3\%}$ (m)	Percentage of cavity length to blade length
$P_{suc.}$ = 0.80 bar, $P_{del.}$ = 2.5 bar H = 33.4m	20	2800	0.40	8.45	3.12	25%
$P_{suc.}$ = 0.60 bar, $P_{del.}$ = 3.2 bar H = 38.32m	20	3000	0.40	8.88	3.85	40%
$P_{suc.}$ = 0.7 bar, $P_{del.}$ = 2.5 bar H = 32m	40	2800	0.40	8.44	4.32	50%
$P_{suc.}$ = 0.52 bar, $P_{del.}$= 3 bar H = 36m	40	3000	0.40	9.22	5.5	70%
$P_{suc.}$ = 0.40 bar, $P_{del.}$= 3.1 bar H = 35.6m	70	3000	0.40	6.4	4.9	> 75 %

Fig. 7-a. (T = 80°C, Q/Q_{opt} = 0.6, N = 3000 rpm)

Fig. 7-b . (T = 28°C, Q/Q_{opt} = 0.7, N = 3000 rpm

Fig. 7 . Developed cavitation corresponding to 3% drop in head

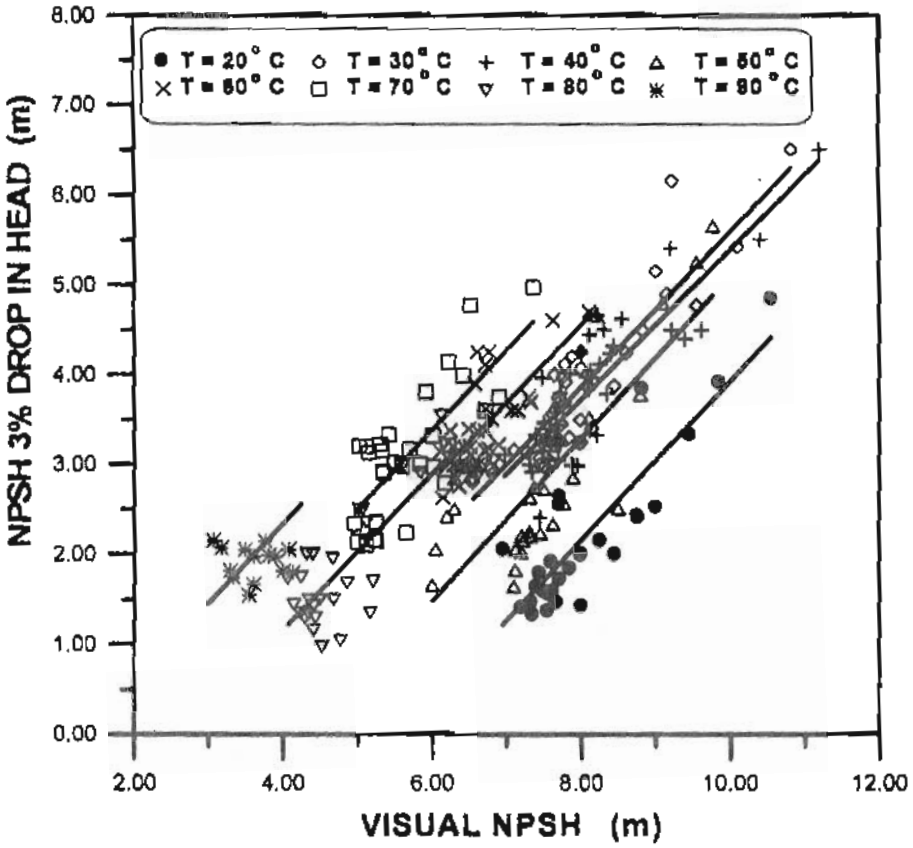

Fig. 8. $NPSH_{3\%}$ in head versus visual NPSH

Table 2: The correlation coefficients and regression lines derived from figure 8.

Data	Correlation coefficient		Linear relationship equation
Independent of operating conditions	0.58		$NPSHi_{vis} = 2.28\ NPSH_{3\%} - 0.966$
Dependent only on water temperature	Min.	0.62	$NPSHi_{vis} = 1.125\ NPSH_{3\%} - 0.05235\ T + 6.3575$
	Max.	0.87	

It can be seen from table 2 that for this data set, which quite comprehensive, that the correlation coefficient for the relationship with account for temperature is better than that with all data. On the basis of these results the best correlation is in terms of water temperature. These findings are the interesting feature of this correlation. This would seem to be a most useful tool in the prediction of the actual condition of the incipient of cavitation for a pump from performance tests as are easy to conduct.

CONCLUSIONS

1) The visual observation of the state of cavitation indicated that at the point where the head drops by 3 percent, developed cavitation was appeared and the incipient of cavitation existed long before the performance is affected. At this point where the head drops by 3% sever cavitation erosion is most likely. Therefore, reliance on 3% drop in head can cause errors in the prediction of performance at design.

2) One of the interesting features of this investigation is that the visual net positive suction head ($NPSH_{i,,vis}$) is well correlated with the net positive suction head corresponding to 3% drop in head ($NPSH_{3\%}$) and the fluid flow temperature. This relation could be defined by an equation of the type:

$NPSH_{i,vis} = 1.125\ NPSH_{3\%} - 0.05235\ T\ (°C) + 6.3575$

The above equation can be used for predicting the actual condition of the incipient of cavitation for a centrifugal pump from performance tests as are easy to conduct.

3) Visual observation and photographs of the state of cavitation at various flow rate ratios and constant values of temperatures and rotational speeds showed that at higher flow rate ratios a pours cavity was found to exist. However, at lower flow rate ratios gaseous cavity was observed. At developed and breakdown condition the colour of cavities changed with changing the water temperature. At lower flow rate ratio ($Q/Q_{opt} < 0.5$) near the start of circulatory flow alternative cavitation commenced.

NOMENCLATURE

$NPSH_{i,vis}$: visual Net Positve Suction Head.

$NPSH_{3\%}$: Net Positve Suction Head corresponding to 3% head drop.

Q : flow rate .

Q_{opt}: optimum flow rate.

T: temperature ^{0}c.

REFERENCES

1. McNulty P. J., and Pearsall, I.S., March 1982, "Cavitation Inception in Pumps", Journal of Fluid Engineering.
2. El-kadi M. A., October 2001, "Cavitation in Centrifugal Pumps Handling Hot Water" Eng. Res. Journal, Helwan University, 77, p.p. 200-216, Egypt.
3. Hirschi R., Dupont Ph., Avellan F., Favre J. N., Guelich J. F., and Parkinson E., December, 1998, "Centrifugal Pump Performance Drop due to Leading Edge Cavitation: Numerical Prediction Compared with Model Rests", ASME Journal of Fluid Engineering, 120, pp. 705- 711
4. Donald P. Sloteman, 2007, "Cavitation in High Energy Pumps - Detection and Assessment of Damage Potential", Proceedings of the Twinty-Third International Pump Users Symposium, pp. 29-38.
5. Wulff, D. L., 2006, "Unsteady Pressure and Velocity Measurements in Pumps ", Education Notes RTO-EN-AVT-143, PP. 1-34, Germany.
6. L. Alfayez, Saudi D. G. Dyson, David Browne, September 2004, "Detection of Incipient Cavitation and the Best Efficiency Point of a 2.2MW Centrifugal Pump using Acoustic Emission", Proceedings of 26th European Conference on Acoustic Emission Testing", 15-17, Berlin.
7 Hofmann M., Stoffel B. Friedrichs J., and Kosyna G., 2001, "Similarities and Geometrical Effects on Rotating Cavitation in Two Scaled Centrifugal Pumps"; www. google. com. eg./.

APPENDIX A

Table A - 1: Experimental values of NPSH corresponding to 3% drop in head

Q/Q_{opt}	$NPSH_{3\%}$ (m)									
	T = 20°C					T = 30°C				
	2600	2700	2800	2900	3000	2600	2700	2800	2900	3000
0.3	2.4	2.52	3.33	3.92	4.85	7.77	5.15	5.42	6.15	6.5
0.4	1.43	2.15	3.12	3.27	3.85	3.5	3.88	4.25	4.5	4.9
0.5	1.38	1.6	2.65	2.85	3.24	3.3	3.72	4.07	3.87	3.4
0.6	1.34	1.48	1.85	2.05	2.64	2.96	3.16	3.18	3.57	3.3
0.7	1.42	1.47	1.6	1.8	2.55	2.81	2.9	2.98	3.25	3.07
0.8	1.45	1.65	1.65	1.73	2.05	2.85	2.9	3.07	3.07	3
1.0	1.47	1.65	1.8	1.82	2.15	3	2.98	3.27	4	3.29
1.05	1.5	1.69	1.85	1.92	2.22	3.22	3.25	3.65	4.11	3.92
1.10	1.52	1.72	2.05	2.12	2.3	3.75	3.45	3.99	4.2	4.25
	T = 40°C					T = 50°C				
0.3	5.4	5.45	5.5	6	6.5	2.5	3.78	4.8	5.25	5.65
0.4	3.79	4.24	4.32	4.62	5.5	2.33	2.55	2.85	3.52	4.66
0.5	3.47	3.4	4.25	3.97	4.5	2.15	2.25	2.72	3.05	3.65
0.6	3	3.33	3.96	3.05	4.32	2.05	2.2	2.62	2.75	3.22
0.7	2.92	2.99	3.5	2.99	3.82	1.65	1.66	2.05	2.42	2.85
0.8	2.4	3.07	3.3	3.25	3.11	1.83	2.02	2.2	2.23	2.5
1.0	3.25	3.15	3.22	3.85	3.98	1.78	2.13	2.22	2.25	2.52
1.05	3.44	3.22	3.66	4.05	4.44	2.25	2.28	2.3	2.35	2.6
1.10	3.8	3.7	4.01	4.12	4.66	2.56	2.62	2.72	2.61	2.75
	T = 60°C					T = 70°C				
0.3	2.41	2.75	4.6	4.7	5.2	4.2	4.77	4.85	4.97	5.02
0.4	2.3	2.48	3.6	3.6	4.92	4.14	4.32	4.52	4.6	4.9
0.5	2.25	2.36	3.38	3.38	4.58	3.81	3.32	3.75	3.8	3.99
0.6	2.2	2.25	3.2	3.2	4.3	3.15	3.22	3.22	3.44	3.17
0.7	2.44	2.2	3	2.98	4.25	2.1	2.8	3.01	3.13	3.35
0.8	2.52	2.6	2.98	3	4.11	2.34	2.88	2.98	3.15	3.4
1.0	2.65	2.85	3.3	3.2	4.25	-	-	-	-	-
1.05	2.99	3.03	3.33	3.38	4.32	-	-	-	-	-
	T = 80°C					T = 90°C				
0.3	-	-	2.91	3.55	-	-	-	-	-	-
0.4	2.5	1.35	1.7	2.88	3	-	-	-	-	-
0.5	1.95	1.04	1.68	2.5	2.35	2.15	2.17	2.21	2.22	2.25
0.6	1.75	1.34	1.44	1.5	1.5	1.98	2.05	2.11	1.99	1.82
0.7	1.74	1.45	1.35	1.3	1.3	1.72	1.98	1.85	1.82	1.95

Table A.2: Experimental values of visual inception

Q/Q_{opt}	NPSHi (m)												
	T = 20 °C								T = 30 °C				
	1500	1800	2100	2600	2700	2800	2900	3000	2600	2700	2800	2900	3000
0.3	-	-	-	8.76	9.00	9.45	9.85	10.5	9	9.22	9.55	10.1	10.82
0.4	7.1	7.23	7.57	8.00	8.25	8.45	8.75	8.88	8	8.45	8.61	8.83	9.15
0.5	6.95	7.1	7.2	7.55	7.67	7.85	8.00	8.00	7.62	7.73	8	8.09	8.15
0.6	6.88	7	7.1	7.35	7.5	7.62	7.71	7.71	6.8	7.11	7.28	7.62	7.85
0.7	6.85	6.9	6.99	7.20	7.33	7.40	7.56	7.70	6.55	6.82	7.52	7.6	7.45
0.8	6.9	6.94	6.99	7.30	7.42	7.49	7.60	7.68	6.55	6.6	6.71	6.82	6.92
1.0	6.94	7	7.1	7.45	7.50	7.55	7.60	7.68	7.45	7.50	7.52	7.65	7.70
1.05	-	7.11	7.2	7.55	7.61	7.66	7.72	7.75	7.64	7.69	7.73	7.78	7.80
1.10	-	-	-	7.67	7.71	7.80	7.85	7.90	7.70	7.74	7.77	7.88	8.00
	T = 40 °C								T = 50 °C				
0.3	-	-	-	9.2	9.4	9.62	10.4	11.2	8.5	8.8	9.1	9.55	9.77
0.4	7.2	7.4	7.65	8.35	8.4	8.44	8.55	9.22	7.62	7.77	7.89	8.11	8.2
0.5	7.13	7.3	7.4	7.51	7.58	8	8.15	8.21	7.22	7.31	7.51	7.6	7.65
0.6	7.05	7.2	7.25	7.32	7.4	7.48	7.7	7.95	7.12	7.2	7.31	7.38	7.41
0.7	6.95	6.95	7.1	7.35	6.2	6.25	7.88	6.98	7.1	7.24	7.24	7.35	7.44
0.8	6.8	6.8	7.05	7.45	7.5	7.65	8.00	8.08	7.12	7.24	7.34	7.44	7.50
1.0	6.9	6.9	7.15	7.51	7.57	7.68	8.10	8.11	7.19	7.29	7.39	7.49	7.50
1.05	-	-	7.3	7.68	7.72	7.77	8.13	8.22	7.24	7.34	7.44	7.54	7.61
1.10	-	-	-	7.73	7.78	7.86	8.26	8.31	7.30	7.38	7.50	7.59	7.72

Cont. table A.2

Q/Q_{opt}	NPSHi (m)												
	T = 60 °C								T = 70 °C				
	1500	1800	2100	2600	2700	2800	2900	3000	2600	2700	2800	2900	3000
0.3	-	-	-	7.15	7.3	7.62	8.11	-	6.22	6.52	6.72	6.9	7.36
0.4	6.02	6.22	6.32	6.5	6.9	7.07	7.33	7.47	5.92	6.01	6.18	6.22	6.42
0.5	5.97	6.07	6.12	6.22	6.52	6.72	6.8	6.82	5.33	5.5	5.66	5.85	6.02
0.6	5.87	5.92	6	6.12	6.25	6.3	6.29	6.42	5.12	5.25	5.34	5.6	5.7
0.7	5.72	5.72	5.82	6.15	6.22	6.37	6.42	6.61	4.96	5.02	5.12	5.15	5.25
0.8	5.52	5.67	5.82	6.35	6.45	6.52	6.62	6.72	5	5.22	5.3	5.35	5.42
1.0	5.72	5.87	5.92	6.47	6.52	6.57	6.72	6.77	-	-	-	-	-
1.05	-	6.02	6.1	6.57	6.62	6.72	6.77	6.87	-	-	-	-	-

	T = 80 °C					T = 90 °C				
	2600	2700	2800	2900	3000	2600	2700	2800	2900	3000
0.3	-	-	5.85	6.12	-	-	-	-	-	-
0.4	5.07	5.17	5.21	5.33	5.62	-	-	-	-	-
0.5	4.67	4.77	4.86	5.02	5.12	3.9	4.08	4.14	4.22	4.3
0.6	4.25	4.35	4.42	4.5	4.68	3.77	3.62	3.77	3.82	4.01
0.7	4.07	4.15	4.24	4.3	4.44	3.62	3.07	3.18	3.3	3.55
0.8	4.32	4.36	4.41	4.4	4.52	3.00	3.21	3.34	3.5	3.61